

## Analysis of the Electron Cyclotron Emission from the Non-Thermal Electron Population Generated by ECRH and ECCD

P. Blanchard, S. Alberti, S. Coda, H. Weisen,

*Centre de Recherches en Physique des Plasmas*

*Association EURATOM - Confédération Suisse, EPFL, 1015 Lausanne, Switzerland*

**Abstract:** Measurements of Electron Cyclotron Emission (ECE) from the high field side (HFS) of the TCV tokamak have been made on plasmas heated by second and third harmonic X-mode Electron Cyclotron Heating (ECH) and Electron Cyclotron Current Drive (ECCD). The ECE increases sharply with the local toroidal incidence angle of the X2 EC beams and with the X2 injected power. The measured ECE spectra are modelled using a bi-Maxwellian describing the bulk and the suprathermal electron populations. Suprathermal temperatures between 10 and 50keV and densities in the range  $1 \cdot 10^{17} - 6 \cdot 10^{18} \text{ m}^{-3}$  are obtained. Good agreement between ECE suprathermal temperatures and energetic photon temperatures, measured by a hard X-ray (HXR) camera, is found. For optically thin X3 LFS ECH injection, reflection of the beam on the inner wall and absorption on the suprathermal electron population partly explain the discrepancy between global energy deposition measurements and first pass calculations.

### Introduction

The TCV tokamak ( $R=0.88\text{m}$ ,  $a<0.24\text{m}$ ,  $B_T<1.54\text{T}$ ,  $I_p<1.2\text{MA}$ ) is equipped with six 0.45MW gyrotrons at the second electron cyclotron frequency (X2) and three 0.47MW gyrotrons at the third harmonic (X3). In the case of a Maxwellian plasma, the optical thickness  $\tau^{Xn}$ , for the X-mode at the  $n$ -th harmonic ( $n \geq 2$ ), is proportional to  $n_e (k_B T_e / m_e c^2)^{n-1}$  [1], X3 absorption is hence much weaker than X2 absorption. In the thermal bulk of TCV plasmas, X2 is optically thick, while X3 is optically thin. Injection of high power electron cyclotron waves in extraordinary polarisation mode in X2 ECCD and/or in X3 ECH injection configuration creates a non-thermal electron population, which increases the single-pass absorption for X3 Low Field Side (LFS) injection [2]. In X2-ECCD preheated plasmas, a seed suprathermal tail is generated and for LFS X3 injection, the X3 EC beam is first partly absorbed on the thermal bulk at the cold resonance and then interacts with the suprathermal population by increasing this non-thermal population and by increasing its absorption efficiency.

### Experimental setup

To study suprathermal electron populations, TCV has been equipped with an ECE radiometer working in the X2 frequency range and connected to a choice of two receiving antennae, on the High Field Side (HFS) of the torus, placed at  $Z=0\text{m}$  and  $Z=0.21\text{m}$ . The ECE radiometer is a X-mode 24 channels super-heterodyne radiometer. It covers the frequency range from 78.5GHz to 114.5GHz, corresponding to the second harmonic of the electron cyclotron fre-

quency at the HFS. The frequency bandwidth of each channel is 750MHz, corresponding to a spatial resolution between 0.4 (edge) and 1 cm (center) for the cold resonance. The radiometer is cross calibrated from Thomson scattering measurements during the ohmic phase of the discharge, prior to ECH and ECCD injections.

The flexibility of the EC heating system allows both the toroidal and the poloidal injection angles to be adjusted<sup>[2]</sup>. The target plasmas used in the experiments reported here have the following parameters:  $I_p=200\text{kA}$ ,  $q_{95}=3.8$ ,  $\kappa=1.31$ ,  $\delta=0.06$ ,  $B_T=1.45\text{T}$ . The X3 power ( $P_{X3}=0.47\text{MW}$ ) and the launching angles (ECH heating) are kept constant, whereas the toroidal and poloidal launching angles of the X2 ECH/ECCD are varied.

For typical densities and temperatures of TCV ( $n_e(0)\sim 2.5\times 10^{19}\text{m}^{-3}$ ,  $T_e(0)\sim 2\text{keV}$ ), the plasma is optically thick (the bulk optical depth  $\tau_b^{X2} > 10$ ) and the ECE radiometer provides a measurement of the electron temperature profile if the distribution function is Maxwellian. In these conditions, the plasma behaves like a black body. The radiation temperature  $T_r$  is defined by  $T_r = 8\pi^3 c^2 I_\omega / \omega^2 (1 - e^{-\tau_b})$ , where  $I_\omega$  is the intensity of the EC radiation at the frequency  $\omega$ . For an optically thick Maxwellian plasma in thermal equilibrium  $T_r=T_e$ : the radiation temperature corresponds to the electron temperature. Concerning the ECE, we will refer to the directly measurable quantity  $T_{ece} = 8\pi^3 c^2 I_\omega / \omega^2$  as the (apparent) ECE temperature.

### Non thermal ECE measurements on TCV

If the plasma is not Maxwellian, e.g. if non-thermal electrons are produced by heating the plasma with EC waves, or if the bulk optical depth is optically thin for the considered radiation,  $T_r$  is no longer equal to the bulk temperature. For plasmas heated by central X2 ECCD,  $P_{X2}=450\text{kW}$  and X3 ECH,  $T_{ece}$  up to six times  $T_b$  have been measured when the X2 local toroidal angle at the resonance is  $+35^\circ$ <sup>[2]</sup>. Under the assumption of a bi-Maxwellian (bulk+suprathermal) electron distribution function, an expression for the local intensity can be obtained as<sup>[3]</sup>:

$$I_\omega = \frac{\omega^2}{8\pi^3 c^2} \left[ T_b \left( 1 - e^{-\tau_b} \right) e^{-\tau_s} + T_s \left( 1 - e^{-\tau_s} \right) \right] \quad (1)$$

with  $T_b$  and  $T_s$  the electron bulk and suprathermal temperatures,  $\tau_b$  and  $\tau_s$  the respective optical depths.

The ECE from suprathermals is frequency-downshifted by the relativistic factor  $\gamma$ . If the radiation is observed from the HFS, this downshifted radiation does not pass through the EC cold resonance and

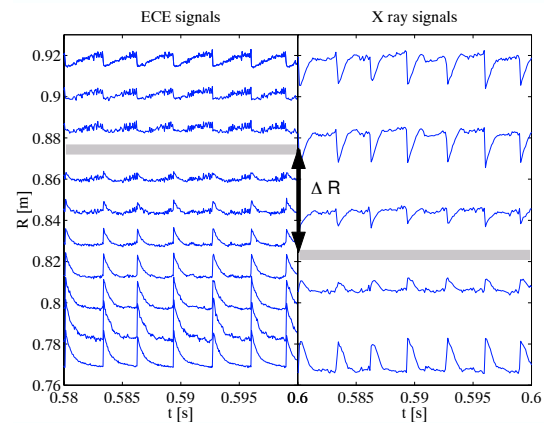


**Figure 1:** Temporal evolution of ECE signals (left) and soft X-ray measurements (right) of shot #21668 with 0.45MW X2 CO-ECCD  $+17^\circ$  local angle and 0.47MW X3 ECH injections. The y-axis represents the radial position of these emissions; in the ECE case, this is calculated considering the cold resonance. The amplitude of the signals is arbitrary. The horizontal gray lines shows the position of the inversion radii for both diagnostics.

is unaffected by the bulk absorption. At any given observation frequency, the intensity of the EC radiation is then the result of a sequence of emission and absorption by electrons from different populations, occurring in different plasma regions. The non-thermal origin of the ECE spectra, in the presence of EC heating, is also clearly demonstrated by the sawtooth activity on the ECE radiometer signals. Comparison of the spatial location of the sawtooth inversion radius, obtained with the ECE radiometer signals and with soft X-ray measurements, clearly shows the effect of the relativistic downshift of the ECE signals emitted by non-thermal population as illustrated in Fig.1. For a radial shift  $\Delta R$ , where  $R$  is the spatial location of the non-shifted event, we obtain the characteristic energy of the non-thermal electrons by  $E=m_e c^2(\Delta R/R)$ . Based on this relation, for the typical heated plasma studied for this paper, the energy estimation of such non-thermal electrons in the X2+X3 phase is between 30 and 45keV while in the X2 phase alone, the energy is between 15 and 35keV.

We simulate the ECE spectrum considering the electron distribution function as a linear combination of two Maxwellians. One of these characterizes the thermal electrons, the other characterizes the suprathermals. The bulk is determined by Thomson scattering measurements while the shapes of the suprathermal temperature and density are obtained by HXR measurements. We assume  $T_s(r)=T_s(0)(1-(r/a)^2)^\alpha$ ,  $n_s(r)=n_s(0)(1-(r/a)^2)^\beta$ ,  $\alpha \in [-0.5, 0.5]$ ,  $\beta \in [6, 10]$ . The central values  $T_s(0)$  and  $n_s(0)$  are the two free parameters that need to be determined in order to satisfy Eq.1. In this equation, the optical depths are calculated in the hot plasma approximation taking into account finite density effects with intermediate temperature effect corrections<sup>[1]</sup>. A result of the application of this method is shown on Fig.2.

The study of optically thin X3 absorbed fraction has shown that the global X3 absorption measured by a diamagnetic loop is larger than predicted by linear calculations made by the code TORAY-GA based on a thermal plasma<sup>[5]</sup>. In particular, a scan of the X2 toroidal injection angle has shown a maxima in the X3 absorbed fraction for an X2 local toroidal angle of  $+25^\circ$  with global absorption measurements of 100% and simulated absorption of 50% indicating a bulk optical depth  $\tau_b^{X3} = 0.7$ . The bi-Maxwellian simulation of the cor-

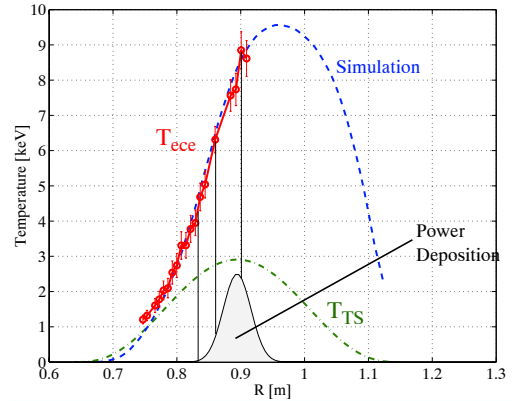


**Figure 2:** Bi-Maxwellian simulation of the ECE spectra for shot # 21732 with 0.45MW X2 CO-ECCD @  $+15^\circ$  and 0.47MW X3 ECH injections.  $\alpha=0$ ,  $\beta=8$ . We used  $T_s(0)=11\text{keV}$  and  $n_s(0)=1.7 \cdot 10^{18}\text{m}^{-3}$ .

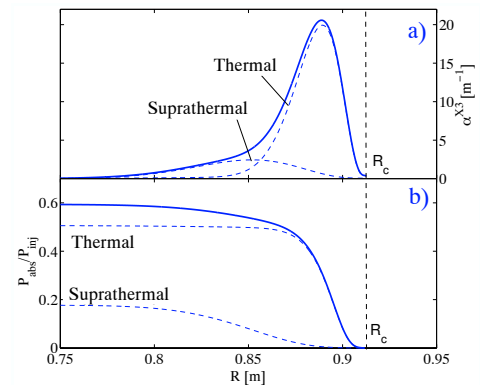


**Figure 3:** **a)** Absorption coefficient for the third harmonic at 118GHz for thermal et suprathermal populations. **b)** Spatial evolution of the X3 absorption by both populations. The thick lines are calculated considering both populations effects.

responding ECE spectra gives  $T_s(0)=14\pm 6\text{keV}$  and  $n_s(0)=1.3\pm 0.4\cdot 10^{18}\text{m}^{-3}$  corresponding to a suprathermal optical depth  $\tau_s^{X3} = 0.2 \pm 0.06$ . The X3 absorption on the thermal and suprathermal populations is  $1 - \exp(-(\tau_s^{X3} + \tau_b^{X3})) = 60 \pm 2.5\%$ .

To study the influence of the EC power on the ECE spectra we carried out a shot-to-shot X2 central power scan from 0 to 1.35MW with  $+15^\circ$  toroidal launcher injection angle before 0.47MW X3 central ECH injection. With X2 heating,  $T_s(0)$  is approximately 7keV and does not depend significantly on the X2 power while  $n_s(0)$  increases linearly from  $1\cdot 10^{17}\text{m}^{-3}$  with  $P_{X2}=0.25\text{MW}$  to  $2\cdot 10^{18}\text{m}^{-3}$  with  $P_{X2}=1.35\text{MW}$ . By contrast  $n_b(0)=1.6\cdot 10^{19}\text{m}^{-3}$  for all shots. Results of the bi-Maxwellian approximation method during X2+X3 combined heating are shown in Fig.4. As the X2 power is increased from 0 to 1.35MW,  $n_s(0)$  increases from  $1.2\cdot 10^{18}\text{m}^{-3}$  to  $5.4\cdot 10^{18}\text{m}^{-3}$ ; at the same time  $T_s(0)$  decreases from 51keV to 12keV. Moreover,  $T_s(0)$  is nearly constant for  $P_{X2}>0.45\text{MW}$ . The suprathermal temperature during X2+X3 injection is in fair agreement with the photon temperature from the HXR camera. We also see that, as the X2 power increases from 0 to 1.35MW with constant X3 power, the central suprathermal optical depth  $\tau_s(0)$  increases from 0.5 to 6.1: the suprathermal population becomes more and more optically thick. The fraction of the electron energy carried by the suprathermals i.e.  $\int n_s T_s dV / \int (n_s T_s + n_b T_b) dV$  is 15% with 0.15MW X2 and increases up to 40% with 1.35MW X2 power.

**Acknowledgments**

This work was partly funded by the Swiss National Science Foundation.

## Acknowledgments

This work was partly funded by the Swiss National Science Foundation.

## References

- [1] M.Bornatici *et al Nucl.Fusion* **23** 1983
- [2] S. Alberti *et al Nuclear Fusion* **42** 42 2002
- [3] P.Blanchard *et al Proc. of the 28th EPS conference on Controlled Fusion and Plasma Physics, Europh. Conf. Abstr.* **23J** 2001
- [4] M.Bornatici & F.Engelmann, *Phys Plasmas* 1 (1994) 189-198
- [5] A.Manini *et al 2002 Plasma Phys. Control. Fusion* **44** 139

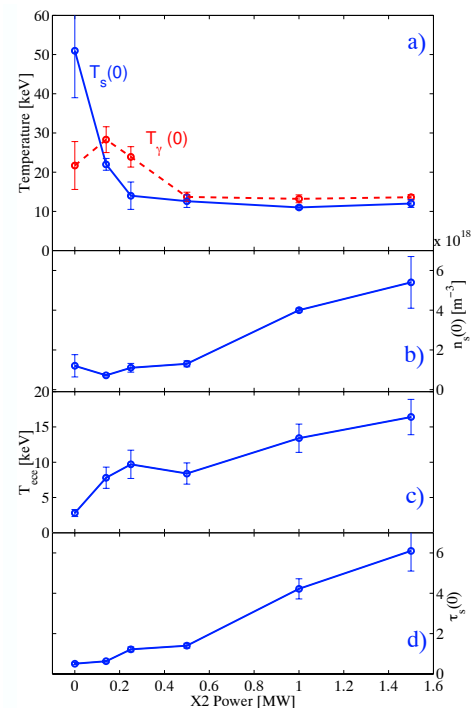


**Figure 4:** Results from the bi-Maxwellian simulations applied on a X2 power scan with 0.47MW X3 ECH power. **a)** Central suprathermal temperature  $T_s(0)$  and photon temperature  $T_g(0)$ . **b)** Central suprathermal density. **c)** Central ECE temperature. **d)** Second harmonic central optical depth for the suprathermals  $\tau_s(0) \propto n_s T_s$